

See discussions, stats, and author profiles for this publication at: <https://www.researchgate.net/publication/270827068>

Sub-chronic Toxicity and Cardiovascular Responses in Spontaneously Hypertensive Rats after Exposure to Multiwall Carbon Nanotubes by Intratracheal Instillation.

ARTICLE *in* CHEMICAL RESEARCH IN TOXICOLOGY · JANUARY 2015

Impact Factor: 3.53 · DOI: 10.1021/tx5004003 · Source: PubMed

CITATIONS

2

READS

143

9 AUTHORS, INCLUDING:



Rui Chen

National Center for Nanoscience and Technol...

28 PUBLICATIONS 150 CITATIONS

SEE PROFILE



Michael T Tseng

University of Louisville

133 PUBLICATIONS 3,067 CITATIONS

SEE PROFILE



Ying Qu

Chinese Academy of Sciences

15 PUBLICATIONS 384 CITATIONS

SEE PROFILE



Chunying Chen

Chinese Academy of Sciences

237 PUBLICATIONS 7,181 CITATIONS

SEE PROFILE

Subchronic Toxicity and Cardiovascular Responses in Spontaneously Hypertensive Rats after Exposure to Multiwalled Carbon Nanotubes by Intratracheal Instillation

Rui Chen,^{†,‡} Lili Zhang,^{†,‡} Cuicui Ge,^{‡,‡} Michael T. Tseng,[§] Ru Bai,[†] Ying Qu,[†] Christiane Beer,^{||} Herman Autrup,^{||} and Chunying Chen^{*,†,‡}

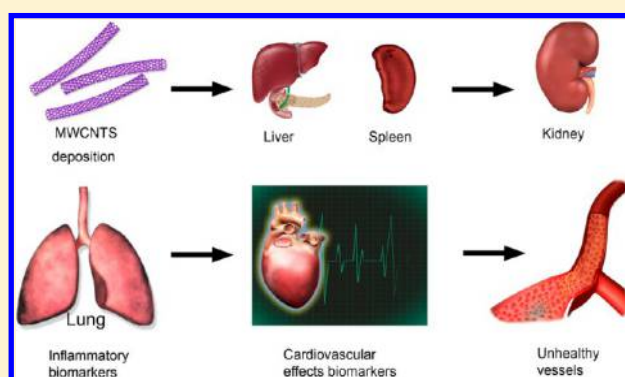
[†]CAS Key Laboratory for Biomedical Effects of Nanomaterials and Nanosafety, National Center for Nanoscience and Technology of China, Beijing 100090, China

[‡]School for Radiological and Interdisciplinary Sciences (RAD-X) & Collaborative Innovation Center of Radiation Medicine of Jiangsu Higher Education Institutions, Soochow University, Suzhou, China

[§]Department of Anatomical Sciences & Neurobiology, University of Louisville, Louisville, Kentucky 40292, United States

^{||}Department of Public Health, Aarhus University, Bartholins Alle 2, 8000 Aarhus C, Denmark

ABSTRACT: The tremendous demand of the market for carbon nanotubes has led to their massive production that presents an increasing risk through occupational exposure. Lung deposition of carbon nanotubes is known to cause acute localized pulmonary adverse effects. However, systemic cardiovascular damages associated with acute pulmonary lesion have not been thoroughly addressed. Four kinds of multiwalled carbon nanotubes (MWCNTs) with different lengths and/or iron contents were used to explore the potential subchronic toxicological effects in spontaneously hypertensive (SH) rats and normotensive control Wistar-Kyoto (WKY) rats after intratracheal instillation. MWCNTs penetrated the lung blood–gas barrier and accumulated in the liver, kidneys, and spleen but not in the heart and aorta of SH rats. The pulmonary toxicity and cardiovascular effects were assessed at 7 and 30 days postexposure. Compared to the WKY rats, transient influences on blood pressure and up to 30 days persistent decrease in the heart rate of SH rats were found by electrocardiogram monitoring. The subchronic toxicity, especially the sustained inflammation of the pulmonary and cardiovascular system, was revealed at days 7 and 30 in both SH and WKY rat models. Histopathological results showed obvious morphological lesions in abdominal arteries of SH rats 30 days after exposure. Our results suggest that more attention should be paid to the long-term toxic effects of MWCNTs, and particularly, occupationally exposed workers with preexisting cardiovascular diseases should be monitored more thoroughly.



INTRODUCTION

Carbon nanotubes (CNTs) are incorporated in a wide variety of consumer products because of their properties. CNTs with single-wall and multiwall structures are termed single-walled carbon nanotubes (SWCNTs) and multiwalled carbon nanotubes (MWCNTs), respectively. CNTs have a high aspect ratio characteristic with diameters typically ranging from 0.4 to 2 nm for SWCNTs and 10 to 100 nm for MWCNTs, while their length may vary from one to several hundred micrometers. In addition, physicochemical characteristics of CNTs such as surface area, agglomeration, structure, and metal purity could be linked to their potential adverse effect on human health and/or the ecosystem.^{1,2} Unfortunately, *in vitro* studies using mammalian cell models often show inconsistent results as they have been conducted in different cell lines, doses, and exposure times. In few *in vitro* studies, CNTs did not display acute toxic effects and exhibited good biocompatibility, although other reports demonstrated that treatment with

CNTs led to the production of reactive oxygen species (ROS) and cellular toxicity.^{3–5} However, *in vivo* pulmonary toxicity studies concluded that CNT exposure caused adverse toxicity effects through inhalation, intratracheal instillation, and pharyngeal aspiration. Both MWCNTs and SWCNTs induced distinct pulmonary inflammation, multifocal granulomas, fibrotic responses, and biochemical/toxicological changes regardless of the type, impurities, and the synthesis process of CNTs.^{6,7} Furthermore, it was reported that highly purified and well-dispersed SWCNTs induced inflammatory responses in the lungs of rats in a dose-dependent manner.⁸ Ingle et al. provided clear evidence that inhaled CNTs can penetrate deep into the lungs, cross the pulmonary epithelium, and enter the

Special Issue: Chemical Toxicology in China

Received: September 30, 2014

Published: January 12, 2015



Table 1. Material Characters Provided by the Supplier^a

full name	abbreviated name	OD (outer diameter) (nm)	length (μm)	purity	dominant metal impurity, content	SSA (m ² /g)	EC (S/cm)
short multiwalled carbon nanotubes	short	<8	0.5–2	>95 wt %	Co, 1.09 wt %	>500	>100
aligned multiwalled carbon nanotubes	aligned	10–20	30–100	>95 wt %	Ni, 1.28 wt %	>165	>100
flash-ignited multiwalled carbon nanotubes	Fe-low	10–50	~50	>95 wt %	Fe, 3.0 wt %	>150	>100
flash-ignited multiwalled carbon nanotubes	Fe-high	10–50	~50	>50 wt %	Fe, 23.0 wt %	>300	>100

^aNA: not available. SSA: special surface area. EC: electric conductivity. Flash-ignited is a special characteristic of CNT products with the possibility of burning under strong flash light.

bloodstream, which will heighten the potential of exposure and toxicological effects to other organs and tissues.⁹ It had been shown that inhaled MWCNTs, which deposit in the lungs, are transported to the parietal pleura, the respiratory musculature, liver, kidney, and heart in a singlet form and accumulate with time postexposure even until day 336.¹⁰

Cardiovascular diseases are the leading cause of deaths worldwide in both high-income and low-income countries. Many toxicological studies show the close link and causal relationship between PM_{2.5} (defined as the particulate matter levels of up to 2.5 μm in diameter) air pollution exposure and cardiovascular morbidity and mortality.^{11–13} For CNTs, Urankar et al. reported that oropharyngeal aspiration of MWCNTs resulted in a time and dose-dependent exacerbation of myocardial infarction when assessed at days 1, 7, and 30 postaspiration.¹⁴ The severity of myocardial injury depended on the form of MWCNTs used. Instillation of SWCNTs in Wistar-Kyoto (WKY) rats was found to alter baroreflex function by affecting cardiovascular autonomic regulation thus contributing to cardiac and arrhythmic events.¹⁵ The spontaneously hypertensive (SH) rat is considered a good animal model of human essential or primary hypertension and has been extensively used to study cardiovascular diseases. The SH rat develops characteristics of cardiovascular diseases similar to those of humans, i.e., higher blood pressure and death due to stroke. Ge et al. reported acute pulmonary and moderate cardiovascular responses in SH rats at days 1 and 3 postexposure to SWCNTs with different metal residues.¹⁶ The coexistence of metal residues in SWCNTs can aggravate the adverse effects. These results suggest a direct influence of CNT exposure on the cardiovascular system. In our present study, we compared the subchronic toxicity of four different kinds of MWCNTs in SH rats by intratracheal instillation at 7 and 30 days postexposure using age-matched normotensive WKY rats as the control. To elucidate the underlying pathophysiological mechanisms linking CNT exposure and its cardiovascular impact, cardiac autonomic regulation and associated peripheral structural changes of the large aorta were also evaluated.

■ EXPERIMENTAL PROCEDURES

Materials and Characterization. Four MWCNTs, labeled short, aligned, Fe-low, and Fe-high, based on their specific characters, were obtained commercially (Chengdu Organic Chemicals Co. Ltd., Chengdu, China). A summary of the MWCNT physicochemical properties is presented in Table 1. Chemical vapor deposition (CVD) was used in the production of the CNTs by using different catalysts, a cobalt-based catalyst for the short ones, a nickel-based catalyst for the aligned ones, and ferrocene for both Fe-low and Fe-high MWCNTs. The contents of dominant metal elements, Co, Ni, and Fe, released from the used catalysts are listed in Table 1. Other metal impurities were much less than 1% (weight) according to the supplier. Except for

Fe-high, all MWCNTs were purified by hydrochloric acid wash after the production process. It had been shown that this nonoxidative treatment does not involve much oxygen content change and the wall defect for MWCNTs but with less help on the dispersion stability when compared to those of other powerful acid washes.¹⁷ High-resolution transmission electron microscopy (HRTEM, Tecnai G2 F20 U-TWIN, FEI Company, USA) was used to characterize the morphology of MWCNTs. The suspension of 1.5 mg/mL MWCNTs was prepared by dispersing MWCNT powders in saline solution containing 0.5% Pluronic F108 (PF108, Sigma-Aldrich Co, USA) and sonicated for 30 min before use. PF108, an excellent biocompatible surfactant, had been selected as dispersants of MWCNTs.¹⁸

Animal Exposure and Experimental Design. Eleven to 12 week old male SH rats (220–250 g) and male WKY rats (370–400 g) were obtained from Vital River Laboratory Animal Technology Co., Ltd. Animals were housed in macrolon cages in an isolated animal room. Experiments were approved according to the Ethics Committee of Animal Care and Experimentation of the National Institute for Environmental Studies, China. Both SH and WKY rats were weighed and randomly allocated into five subgroups (*n* = 6). A dose of 600 μg/kg MWCNT in 200 μL saline was administered once a day for two consecutive days (a total dose of 1.2 mg/kg) by using a nonsurgical intratracheal instillation after anesthesia by ether. SH or WKY rats were treated with the four types of saline-suspended MWCNTs particles and one group of each was treated with saline as a control, respectively. The rats were sacrificed at days 7 and 30 after the last exposure. At necropsy, animals were anesthetized with 40 mg/kg intraperitoneal sodium pentobarbital and terminated by exsanguination via the abdominal aorta. The tissues and organs such as the heart, liver, spleen, kidneys, and lung were excised and weighed accurately. After weighing the body and tissues, the organ coefficients of the heart, liver, spleen, lung, and kidneys to body weight were calculated as the ratio of tissue (wet weight, mg) relative to body weight (g).

Electrocardiogram Monitoring. Electrocardiogram (ECG) data and the biophysical parameters including blood pressure and heart rate were measured by the noninvasive method of tail cuff plethysmography (BIOPAC MP-100, USA). The measurements were performed on 6 rats in each group including the control and MWCNT-treated groups 1 day before and after the two consecutive days of treatment with MWCNTs, and every week after treatment.

Biochemical Analysis of Bronchoalveolar Lavage Fluid and Serum Samples. Biochemical analysis of bronchoalveolar lavage fluid (BALF) and blood samples were collected. The biomarkers of lactate dehydrogenase (LDH), tumor necrosis factor-α (TNF-α), and Clara cell 16 (CC16) protein in BALF were analyzed to assess pulmonary toxicity by enzyme-linked immunosorbent assay (ELISA) tests. Endothelin-1 (ET-1), angiotensin I-converting enzyme (ACE), fibrinogen, and von Willebrand factor (vWF) in citrate plasma and C-reactive protein (CRP) and inter cellular adhesion molecule-1 (ICAM-1) in serum samples were determined as previously described.¹⁹ Briefly, the right lungs of rats were lavaged three times with a volume of phosphate-buffered saline (PBS, pH 7.4) according to 27 mL/kg body weight. Then, the recovered BALFs were centrifuged, and the precipitates were collected for cell counts and differentiation. For differential cell counts of polymorphonuclear neutrophilic leukocyte (PMN), cytopsin slices were made and stained with Giemsa, and at least 200 cells were counted. The BALF

supernatant was used for cellular toxicity evaluation by ELISA. Serum or plasma samples were collected following standard operation procedures. The fibrinogen, ET-1, ACE, and vWF in citrate plasma and ICAM-1, TNF- α and CRP contents in serum were measured using ELISA kits. All related ELISA kits were provided by Usen Life Science Inc., Wuhan, China. Then, the absorbance was measured by a microplate reader (Tecan Infinite M200, Tecan, Durham, USA).

Histopathological Examination. The histopathological test was performed using standard laboratory procedures. Briefly, the organ tissues were embedded in paraffin blocks, then cut in 4- μ m-thick sections, and mounted onto the glass slides. After hematoxylin–eosin (HE) staining, the pathological changes of tissues were observed under an optical microscope (Leica DM4000M, Germany). The identity and analysis of the pathology sections were blind to the pathologist.

Transmission Electron Microscope Observation. For the transmission electron microscope (TEM) examination, the fresh isolated tissue samples were immersed in 2.5% glutaraldehyde at 4 °C. After sufficiently washing with PBS, they were fixed with 1% osmium tetroxide, dehydrated in a graded series of ethanol, and embedded in Araldite, polymerized for 24 h at 37 °C. Ultrathin sections (50 nm) were cut with an ultramicrotome (LKB-V, Sweden), stained with uranyl acetate and lead citrate, and finally observed with a TEM (H-600, Hitachi, Japan) or a Phillips CM-10 electron microscope equipped with an LaB6 cathode (Phillips Electronic Instruments Co. Eindhoven, Netherlands) at 80 kV by an independent pathologist.

Statistical Analysis. The data were expressed as mean \pm standard deviation (mean \pm SD). All of the statistical analyses were implemented using SPSS v19.0 (SPSS Inc., Chicago, USA). A two-way analysis of variance following a posthoc least-significant difference multiple comparison test and Newman-Keuls Test were used to compare animal groups of the same model and the same time point in the study. $p < 0.05$ was considered statistically significant.

RESULTS

Characteristics and Morphology of MWCNTs. The short MWCNTs show thin and short tubes with lengths ranging from 0.5 to 2 μ m and diameters less than 8 nm as well as a bundled characteristic under TEM (Figure 1A). The

aligned MWCNTs were much longer with lengths between 30 and 100 μ m and with diameters ranging from 10 to 20 nm. The aligned MWCNTs usually kept their alignment state (Figure 1B). The length and diameter of Fe-low and Fe-high MWCNTs are similar either claimed by the vendors or illustrated in the HRTEM images (Figure 1C, D). Metal catalysts are essential in the mass production of CNTs by the chemical vapor deposition technique. The metal impurities could be clearly seen along the outer side of Fe-high MWCNTs, while they were only found at the terminal part of Fe-low MWCNTs.

Effects on Organ Coefficients. Table 2 shows the body weight and coefficients of organs relative to body weight at days 7 and 30 after intratracheal instillation. MWCNT treatment had no influence on the body weight and organ coefficients of the heart, spleen, and kidney in both WKY and SH rat models. At day 7 postexposure, the organ coefficients of the liver were significantly decreased when comparing MWCNT treated groups to the control in the two rat models, except for the Fe-low MWCNT treated WKY animals, which showed no significant effect. However, as evidenced by the significant increase of the lung coefficient, lung edema was induced in all treatment groups especially in SH rats at day 7 postexposure, while no effect was seen in WKY rats treated with short MWCNTs, in particular. The toxicity of Fe-low was much higher than that of other MWCNTs when considering the changes of the lung coefficient. The decrease in organ coefficients of the liver and increase of lung coefficients illustrates that the serious damage in these organs are from MWCNT exposure. Even at 30 days postexposure, the lung and liver still showed poor recovery with significant differences in organ coefficients in most treated groups, especially in the Fe-high and Fe-low groups. However, the short and aligned MWCNTs show much damage to the rats at day 7 but with no more durable influences as evidenced by the results of day 30 (Table 2).

Subchronic Toxic Effects after MWCNT Exposure. LDH activity, PMN influx, and albumin levels in the BALF were used as parameters of the pulmonary damage (Figure 2). Figure 2A shows significant up-regulation of LDH activity throughout all checked time points in SH rats, which suggests serious cellular damage in the respiratory system. In WKY rats, the situation of pulmonary damage was similar to the SH rat model except for some improvement in Fe-low and Fe-high MWCNT treated groups at day 30. Figure 2B shows the number of PMNs was significant either in SH or WKY rats, especially exposure to the short CNTs resulted in more serious damage than other MWCNTs. With normal structure and function, the alveolar membrane and pulmonary capillary membrane can prevent the passing of albumin. High concentration of albumin in the BALF therefore suggests injury of the alveolar epithelial barrier. In WKY rats, the albumin level was only found to be significantly increased at day 7 after exposure to MWCNTs, whereas SH rats showed a significant increase at days 7 and 30 postexposure (Figure 2C). Taken together, these results suggest that SH rats may require a longer time for recovery after MWCNT exposure compared to normal rats. An elevated TNF- α level could be detected at day 7 but not at day 30 postexposure in all MWCNT treated groups of SH rats (Figure 2D), while TNF- α was not increased in WKY rats at days 7 and 30. The 16 kDa CC16 protein is secreted in the terminal bronchioles and forms a sensitive marker for the detection of lung hyperpermeability, especially

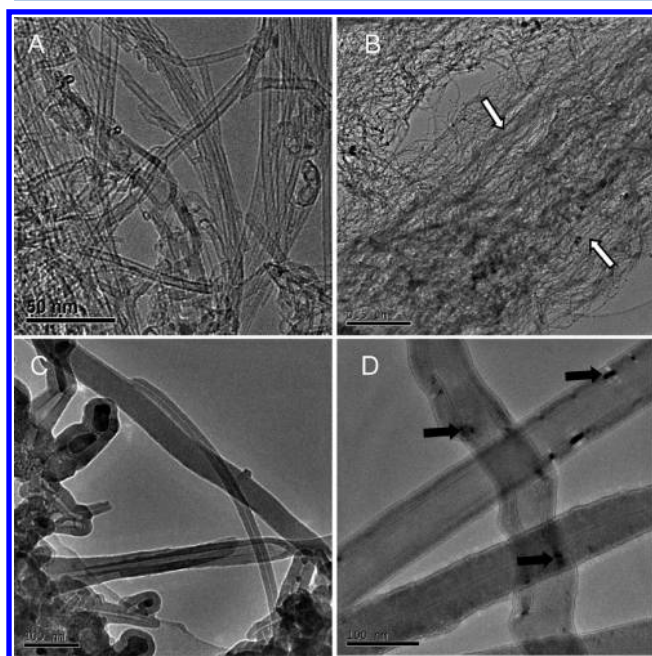


Figure 1. TEM characterization of MWCNTs. (A) Short MWCNTs; (B) aligned MWCNTs; white arrows show the aligned character; (C) Fe-low MWCNTs; and (D) Fe-high MWCNTs; black arrows point to the metal residues along the outer side of tubes.

Table 2. Body Weight and Organ Tissue Coefficients (mg/g, Relative to Body Weight) after Intratracheal Instillation of MWCNTs at 7 and 30 Days^a

groups	body weight (g)	heart	liver	spleen	lung	kidneys
WKY Rats (7 Days after Treatment)						
control	409.3 ± 22.6	3.4 ± 0.4	37.0 ± 3.5	2.5 ± 0.3	7.7 ± 0.4	7.2 ± 0.8
short	401.7 ± 21.8	3.3 ± 0.2	33.6 ± 1.3 ^b	2.6 ± 0.5	8.3 ± 0.8	7.4 ± 0.4
aligned	409.8 ± 27.3	3.3 ± 0.3	32.2 ± 2.6 ^b	2.5 ± 0.2	8.8 ± 1.2 ^b	7.2 ± 0.5
Fe-low	409.6 ± 21.5	3.5 ± 0.4	35.1 ± 3.8	2.5 ± 0.3	10.4 ± 1.0 ^c	7.7 ± 0.6
Fe-high	414.3 ± 23.8	3.3 ± 0.3	30.8 ± 2.2 ^b	2.4 ± 0.3	8.8 ± 1.0 ^b	7.4 ± 0.6
WKY Rats (30 Days after Treatment)						
control	431.9 ± 21.4	3.0 ± 0.3	29.0 ± 2.2	2.2 ± 0.5	6.8 ± 0.8	6.3 ± 0.5
short	451.3 ± 57.4	3.0 ± 0.3	30.8 ± 1.8	2.2 ± 0.2	7.5 ± 0.8	6.2 ± 0.5
aligned	458.2 ± 44.0	3.2 ± 0.3	29.9 ± 2.1	2.2 ± 0.5	6.8 ± 1.0	6.4 ± 0.5
Fe-low	448.1 ± 23.7	3.1 ± 0.2	29.5 ± 2.7	2.3 ± 0.1	8.7 ± 0.9 ^d	6.5 ± 0.6
Fe-high	440.1 ± 32.3	3.2 ± 0.3	27.8 ± 1.4	2.1 ± 0.3	7.9 ± 0.7 ^b	6.1 ± 0.2
SH Rats (7 Days after Treatment)						
control	268.9 ± 7.7	4.4 ± 0.2	34.8 ± 2.6	2.1 ± 0.1	8.4 ± 0.9	7.6 ± 0.2
short	261.6 ± 16.3	4.7 ± 0.3	31.5 ± 2.2 ^b	2.2 ± 0.3	10.3 ± 0.8 ^b	7.5 ± 0.2
aligned	264.7 ± 21.1	4.4 ± 0.3	30.3 ± 2.3 ^b	2.1 ± 0.3	10.9 ± 1.7 ^b	7.5 ± 0.3
Fe-low	257.7 ± 16.0	4.6 ± 0.3	31.6 ± 3.3 ^b	2.1 ± 0.3	16.4 ± 2.8 ^e	7.7 ± 0.2
Fe-high	265.1 ± 13.4	4.5 ± 0.3	29.9 ± 2.9 ^b	2.1 ± 0.2	14.2 ± 3.7 ^e	7.6 ± 0.3
SH Rats (30 Days after Treatment)						
control	318.2 ± 13.0	4.3 ± 0.2	33.3 ± 1.4	2.1 ± 0.1	8.1 ± 0.5	7.4 ± 0.4
short	300.6 ± 38.1	4.6 ± 0.8	33.1 ± 4.7	2.3 ± 0.3	8.6 ± 0.9	7.7 ± 1.3
aligned	310.0 ± 25.0	4.2 ± 0.3	32.7 ± 0.9	2.2 ± 0.2	8.9 ± 0.5	7.4 ± 0.3
Fe-low	315.2 ± 19.1	4.4 ± 0.3	31.2 ± 0.5	2.0 ± 0.1	11.9 ± 0.8 ^c	7.0 ± 0.3
Fe-high	308.4 ± 33.7	4.4 ± 0.2	30.4 ± 1.3 ^b	2.1 ± 0.1	9.0 ± 1.2	7.2 ± 0.3

^aStatistical analyses were implemented within the same animal model and the same time point after exposure. ^b $p < 0.05$ vs control group. ^c $p < 0.05$ vs other treatment groups. ^d $p < 0.05$ vs control and aligned groups. ^e $p < 0.05$ vs control, short and aligned groups.

when the injury happens at deeper sites of the lung. To our surprise, noticeably elevated concentrations of CC16 in BALF was detected in SH and WKY rats 30 days postexposure in all MWCNT treated groups except for WKY rats treated with short MWCNTs. Figure 2E shows that exposure to Fe-high MWCNTs resulted in an increase of CC16 protein level in SH rats already at day 7 postexposure.

Responses of Blood Pressure and Heart Rate to MWCNTs Exposure. ECG monitoring at different time points was undertaken before and throughout the MWCNT intratracheal instillation exposure experiment. MWCNT treatments did not influence the blood pressure and cardiac rhythm of WKY rats (Figure 3A,C). However, in SH rats, a transient decrease of the blood pressure 24 h postexposure and a more obvious long-term decrease of the heart rate were found, which means that stress response in the cardiovascular system could easily be detected in the SH rat model (Figure 3B, D). Compared to the aligned and Fe-high MWCNT treated groups that showed slightly persistent decrease of the heart rate throughout the experiment, exposure to short and Fe-low MWCNTs had less impact on the heart rate of SH rats with a quick recovery (Figure 3D).

Cardiovascular Effects in MWCNT Treated Rats. Blood biochemical assays showed significant increase in white blood cells, lymphocytes, and neutrophils, while no significant changes were observed in other hematological parameters in blood samples of SH and WKY rats at days 7 and 30 after exposure (data not shown). ET-1 concentrations were significantly increased in the blood of all MWCNT treated groups of SH rats at day 7 postexposure but returned to the normal level at day 30. However, WKY rats treated with aligned MWCNTs still showed an elevated ET-1 level at day 30 (Figure

4A). The concentration of ACE was significantly increased by all tested MWCNT types at day 30 postexposure in SH rats, while it was only increased in WKY rats treated with aligned MWCNTs (at days 7 and 30 postexposure) or Fe-high MWCNTs (day 7 postexposure) (Figure 4B). Except for short MWCNTs, the exposure led to elevated production of CRP in SH rats at the 30 day time-point and in WKY rats treated with Fe-high MWCNTs at days 7 and 30. This suggests a persistent inflammation and poor recovery in these scenarios (Figure 4C). Fibrinogen is a predictor of cardiovascular risk. At day 7 postexposure, significantly increased fibrinogen levels were found in all MWCNT treated SH rat groups but not in WKY rats (Figure 4D). Fibrinogen was elevated in WKY rats treated with Fe-high MWCNTs at day 30 suggesting potent long-term pulmonary injury. No significant change was observed in the levels of vWF and ICAM-1 in both rat models, except for Fe-high MWCNTs that showed significant increase of vWF in WKY rats at day 7 after exposure (Figure 4E,F).

Bioaccumulation and Systemic Translocation of MWCNTs in SH Rats at Day 30 post Exposure. It has been reported that CNTs can penetrate deeply into the lung, cross the pulmonary epithelium, and enter the bloodstream. In this study, traces of CNTs were observed by TEM in the organs of SH rats after exposure for 30 days. Figure 5 shows that MWCNTs accumulated in the lungs. MWCNTs were also found in the liver, kidney, and spleen but not in the heart or aorta. Typically, the hepatocytes of the liver and macrophages of the lung and spleen are involved in the phagocytosis of MWCNTs (Figure 5A–D). Compared to the control where hepatocytes exhibit large arrays of rough endoplasmic reticulum (ER) with occasional wisps of smooth ER, MWCNT exposure led to small patches of tubular shaped inclusions partially

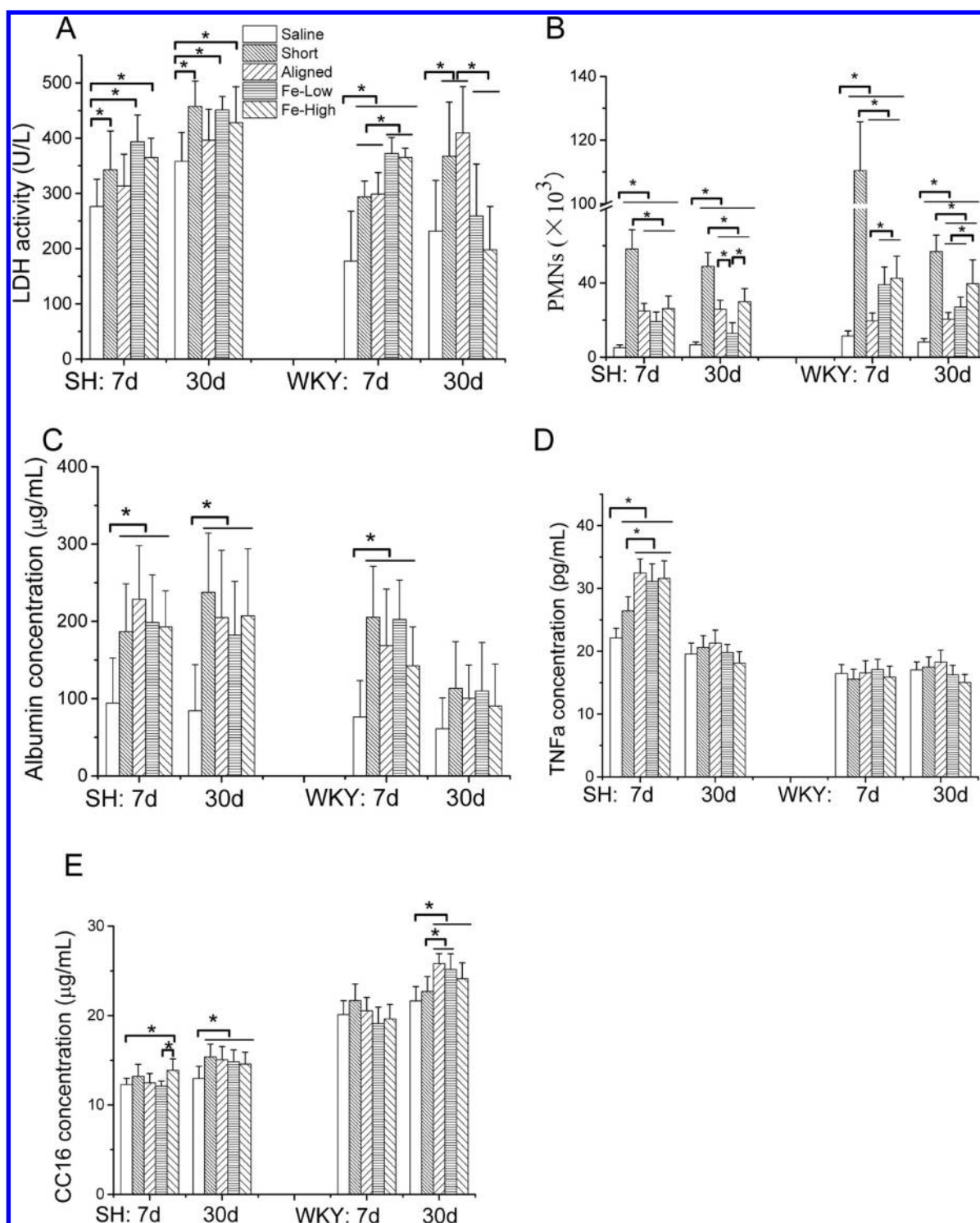


Figure 2. Biomarkers in lung BALF measured at days 7 and 30 after exposure to MWCNTs. (A) LDH activity, (B) PMN number, (C) albumin, (D) TNF- α , and (E) CC16, * $p < 0.05$ vs the saline group at the same time point.

darkened by the iron particles in the CNTs. The uptake in the spleen is demonstrated by comparing the control with the phagocytic accumulation of iron-containing MWCNTs (Figure 5E,F). High accumulation of the compacted tubular element is only found in the spleen of the MWCNTs treated group. Similarly, occasional electron dense particles are only detected in the pedicels of the podocytes after MWCNT treatment in the kidney (Figure 5G,H).

Structural Changes in Large Arteries of SH Rats at Days 7 and 30 after MWCNT Exposure. We investigated the exposed rats for vascular lesions as a sign of long-term inflammation that, as suggested by our results, may cause vascular complications in SH rats. Morphological alterations in abdominal arteries from SH rats were evaluated by HE staining as shown in Figure 6. Generally, the endothelial lining covering the smooth muscle layer in the tunica media appeared to be tightly adhered in control and saline groups (Figure 6A,B).

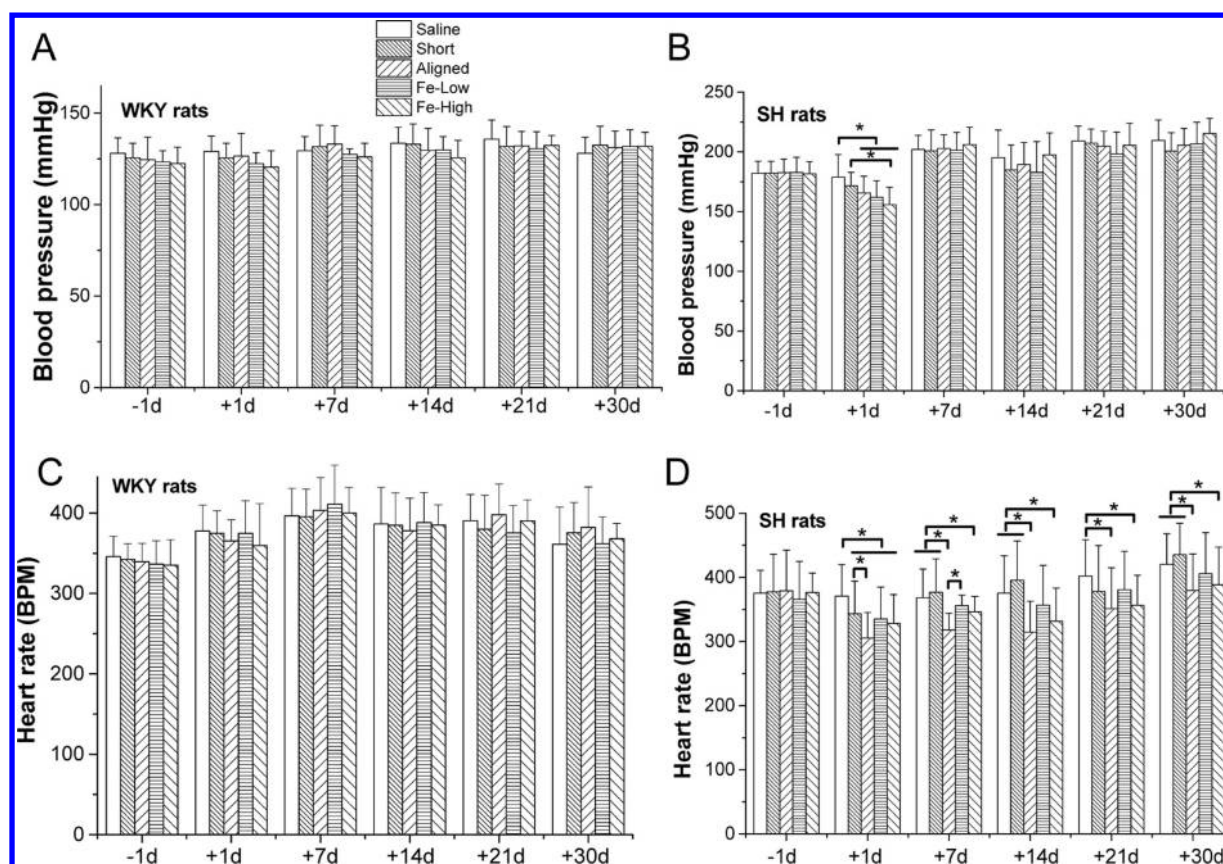


Figure 3. Effects of different MWCNTs on blood pressure and heart rate after intratracheal instillation. (A) Blood pressure of WKY rats, (B) blood pressure of SH rats, (C) heart rate of WKY rats, and (D) heart rate of SH rats. The two consecutive days of MWCNTs exposure are marked as zero. In each experimental group, six animals were used for blood pressure and heart rate measurements. The bars represent the mean \pm SD from three independent measurements, * $p < 0.05$ vs the saline group at the same time point.

However, the lesions including hyperplasia of smooth muscle cells, inconsistency of the endothelium, and even the disorder of elastic laminae were found in SH rats at days 7 and 30 postexposure to MWCNTs. Comparatively, except for the aligned ones, all MWCNTs showed quite serious lesions at the 30 day time-point (Figure 6C–J). No obvious lesions were found in WKY rats (data are not shown).

DISCUSSION

In our previous report, we demonstrated that exposure to MWCNTs can cause acute and strong lung injury including inflammation, oxidative stress, and toxicity in the respiratory system of SH rats. Furthermore, the acute systemic damages in the liver and myocardial tissue occurred along with pulmonary injury at the same time.¹⁹ Subsequently, this study focused on the subchronic toxicological effects and the possible *in vivo* bioaccumulation of MWCNTs. The SH rat, which is highly susceptible to cardiovascular effects due to high blood pressure, was used to evaluate the toxicity and potential cardiovascular effects resulting from MWCNT treatment. We hypothesized that SH rats would be at increased risk of cardiac lesions upon MWCNT exposure. Our results show that the lung and liver are the major target organs for MWCNT induced toxicity following intratracheal instillation. Severe damage to the lung and even to the liver was indicated through changes in the organ coefficients, although the rat body weight was not greatly influenced at days 7 and 30. The subchronic lung injury includes probably inflammation, oxidative stress, and toxicity as

measured by toxicity markers in the BALF such as LDH, PMNs influx, albumin, TNF- α , and CC16. It shows that SH rats usually underwent more serious damage and with slower recovery compared to those of WKY rats. For different characteristics of MWCNTs, the short ones illustrated an extremely high increase in the number of PMNs in BALF than the other ones. However, the short ones had a quick recovery characteristic when considering the TNF- α and CC-16 data especially at 30 days, which may be the reason for the quick elimination of short length CNTs from the body.⁴

Epidemiological studies have shown that cardiovascular diseases with increased morbidity and mortality are linked to the inhalation exposure of particles from air pollution.¹¹ Our results in SH rats showed a transient decrease in blood pressure and a quick recovery after exposure to all four kinds of MWCNTs, which is in accordance with previous studies on combustion source PM exposure.²⁰ No transient stress response in blood pressure could be found in the WKY rats. From the ECG data, no solid evidence for morphology changes of the T-wave and ST segment as a result of the MWCNT treatments was observed. However, animal groups treated with MWCNTs including aligned and Fe-high MWCNTs showed a persistent decrease in the heart rate throughout the entire study, whereas exposure to the short and Fe-low MWCNTs was followed by a relatively quick recovery. Furthermore, aligned and Fe-high MWCNTs led to significantly higher ET-1 and fibrinogen levels in WKY rats than those in the other two CNTs. These results illustrate that the different physicochem-

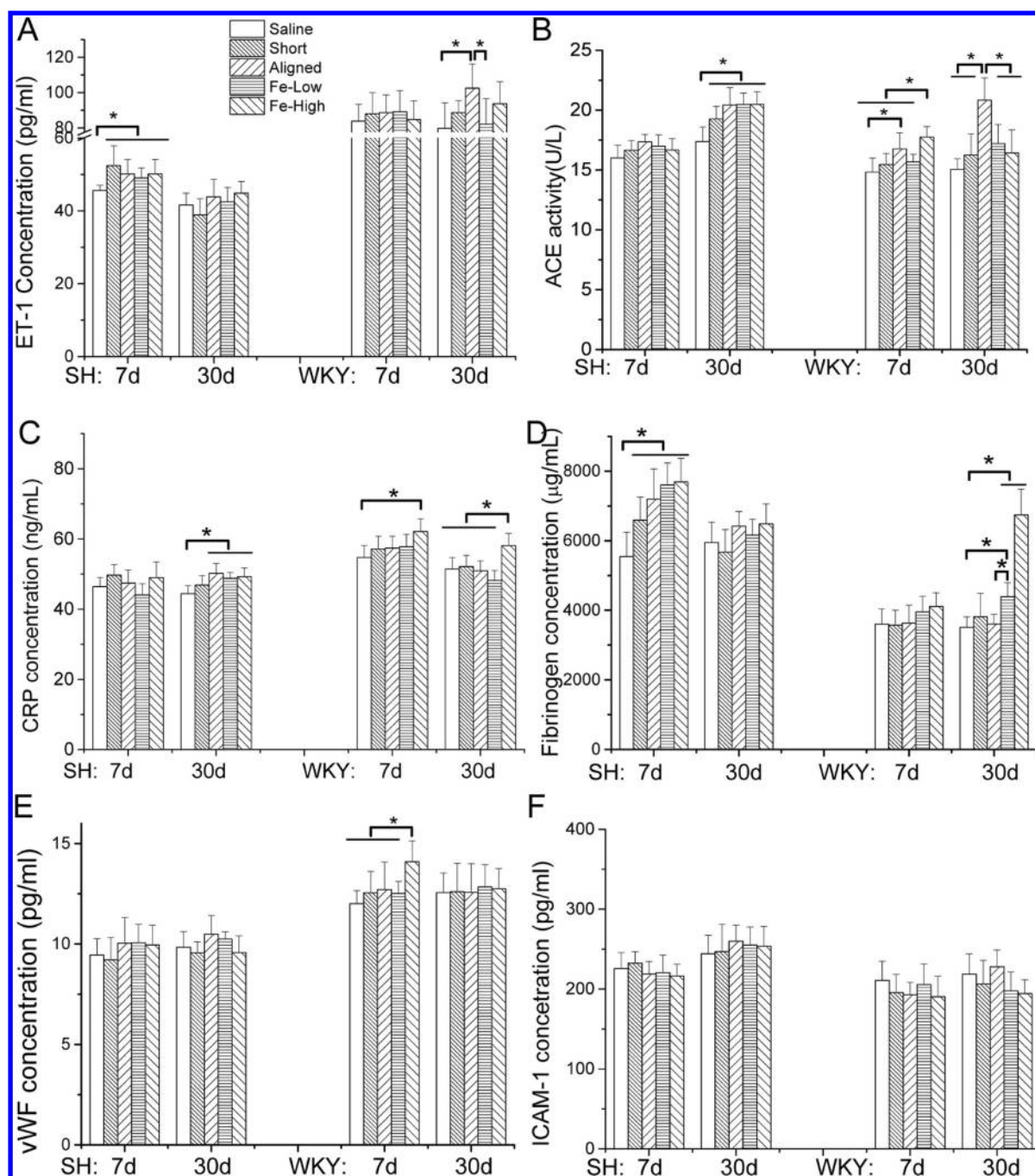


Figure 4. Biomarkers for cardiovascular effects in blood samples measured at days 7 and 30 after exposure to MWCNTs. (A) ET-1 activity, (B) ACE, (C) CRP, (D) fibrinogen, (E) vWF, and (F) ICAM-1, $*p < 0.05$ vs the saline group at the same time point.

ical properties of MMCNTs here studied may lead to different damage intensities and toxicological responses *in vivo*. As a central part of the respiratory system, the lung has the largest epithelial surface area of the human body that is in direct contact with the outside atmosphere. Our results suggest that inhalation of MWCNTs may lead to longer and a more serious injury situations to the pulmonary system than previously anticipated.^{16,21}

It has been shown that there is cross-talk between the lung and systemic circulation during carbon nanotube respiratory exposure. Acute local and systemic responses are activated and can be characterized by a blood gene and protein expression signature, which can be used as a biomarker.²² Our study

showed significant increases of ET-1, ACE, fibrinogen, and CRP levels at days 7 and/or 30 postexposure especially in the plasma of SH rats, which strongly suggests that the normal function of the cardiovascular system of SH rats is more easily disturbed than that of WKY rats. The SH rats showed persistent response to MWCNT treatments in terms of inflammation, tissue injury or necrosis. These conditions cause the release of internal cytokines that trigger the synthesis of CRP and fibrinogen by the liver. ET-1 is the most potent vasoconstrictive substance known and plays a key role in vascular homeostasis. These elevated cardiovascular effect markers suggest an increased risk of high blood pressure (hypertension), peripheral vascular thrombosis, and other heart

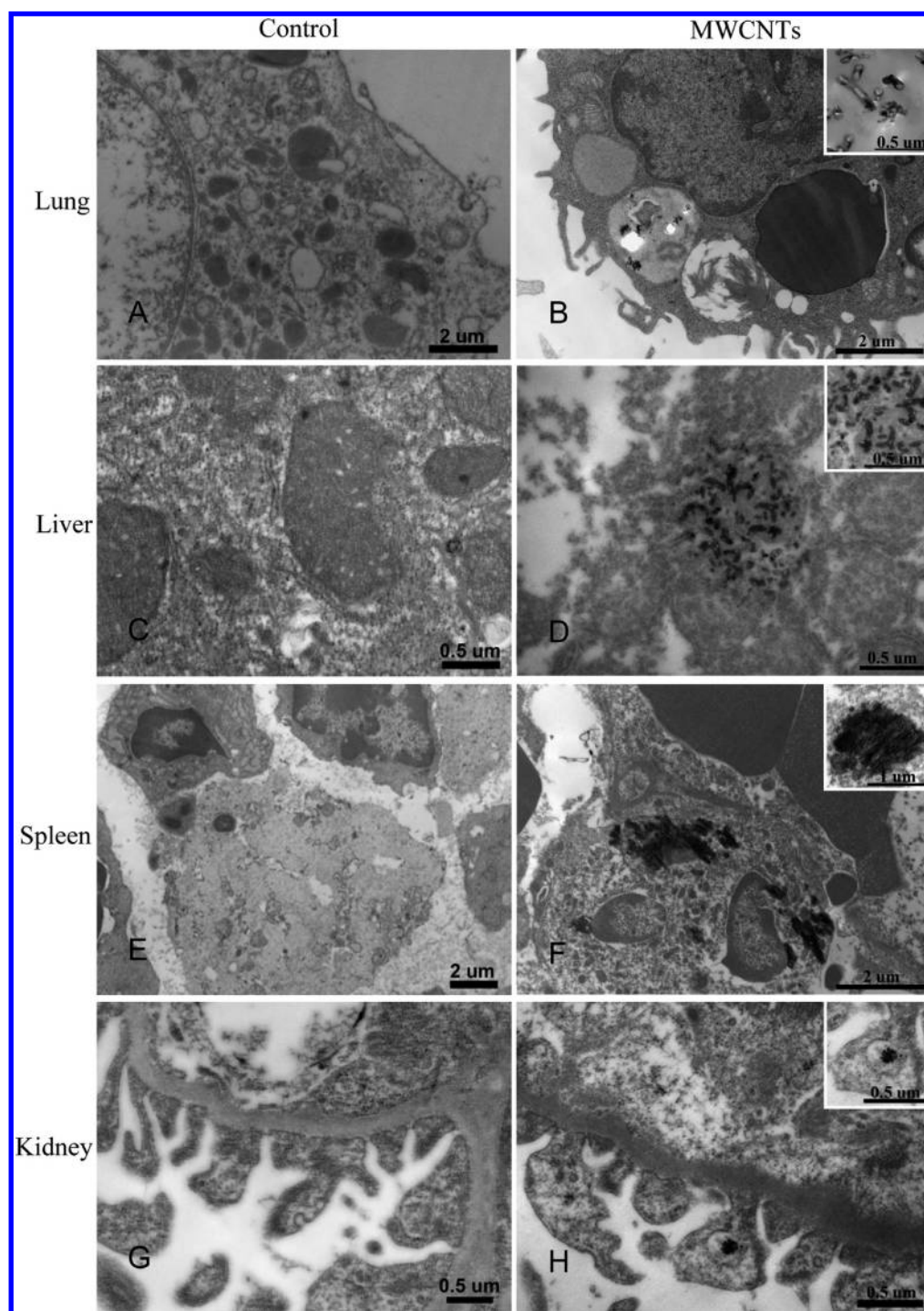


Figure 5. Representative TEM images with clear evidence of MWCNT accumulation in tissues of SH rats after exposure for 30 days. (A) Control lung tissue, (B) alveolar macrophage phagolysosome containing Fe-high MWCNTs with iron core in lung tissue, (C) control liver tissue, (D) Fe-high MWCNTs accumulated in the liver, (E) control spleen tissue, (F) phagocytic accumulation of Fe-high MWCNTs in the spleen, and (G) control kidney tissue. (H) Electron dense particles are only detected in the pedicels of the podocytes from the kidney tissue of the Fe-high MWCNT treated group.

diseases. No changes in the levels of vWF and ICAM-1 were observed, although vWF was elevated at day 7 in Fe-high MWCNT treated animals. The internal dysfunction in SH rats is serious even at days 7 and 30 postexposure where the animals experience a decrease in heart rate. However, no significant change was found in blood pressure. Cardiovascular diseases, especially hypertension, can accelerate the processes of vascular hypertrophic remodeling and increase of stiffness which usually

happens with aging.²³ On the contrary, changes in the vascular structure play an important role in the development of cardiovascular diseases. So the hypertension has a close link to the peripheral vascular structure, which is important for maintaining the normal function of the body.^{24,25} Vasoactive substances usually cause chronic vascular injuries, although sometimes they may cause acute medial lesions without significant early endothelial damage. In present study, the

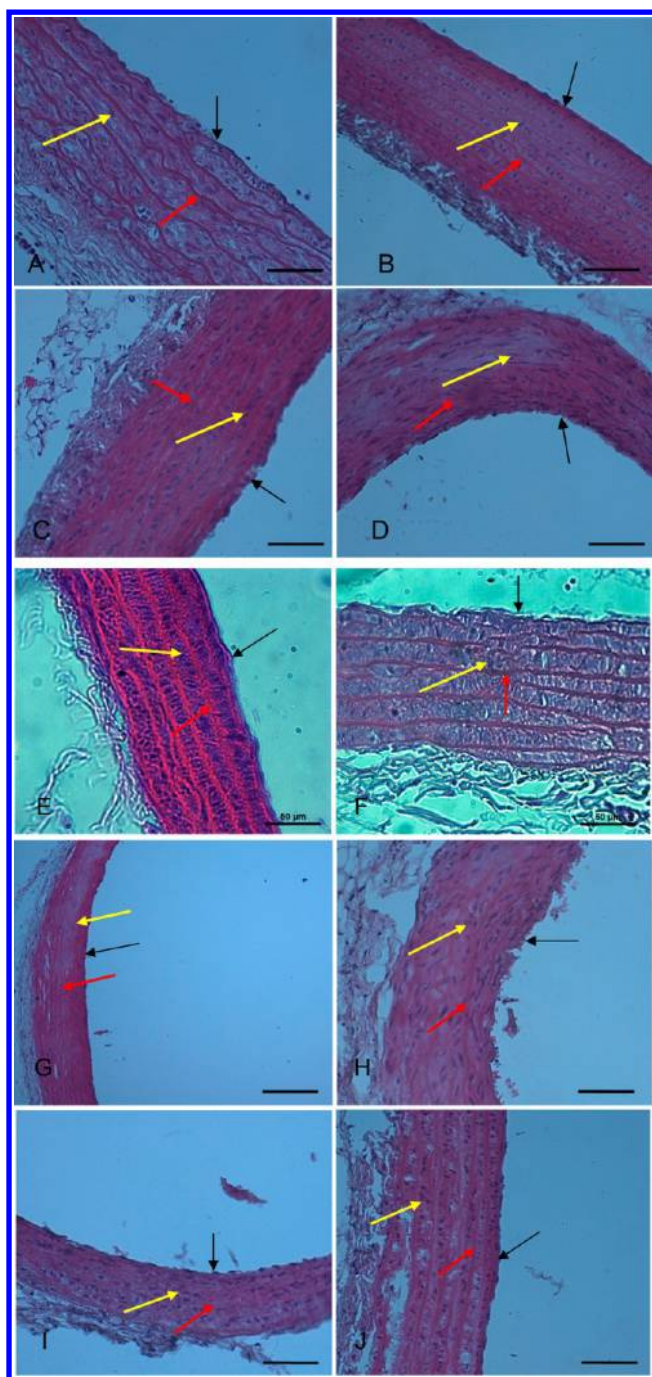


Figure 6. Morphological changes in abdominal arteries of SH rats at days 7 and 30 after exposure to MWCNTs. (A) Normal control, (B) saline control, 30 days, (C) short MWCNTs group, 7 days, (D) short MWCNTs group, 30 days, (E) aligned MWCNTs group, 7 days, (F) aligned MWCNTs group, 30 days, (G) Fe-low MWCNTs group, 7 days, (H) Fe-low MWCNTs group, 30 days, (I) Fe-high MWCNTs group, 7 days, and (J) Fe-high MWCNTs group, 30 days. Yellow arrows point to the smooth muscle cell in the medial layer of the artery. Red arrows point to the elastic laminae. Black arrows show the endothelium. Bars = 50 μ m.

lesions on abdominal arteries in SH rats were found along with the changes of toxic and cardiovascular response markers that presumably originated from MWCNTs exposure, whereas the phenomenon in WKY rats was not so pronounced. Diffuse medial fibrinoid necrosis is the primary reason for vascular

injury when elevated levels of vasoactive substances are present simultaneously with the hypertension background of SH rats.²⁶ In this study, WKY rats have also been found to have high levels of cardiovascular effect markers especially when treated with Fe-high or aligned MWCNTs. This suggests that the biological and toxicological effects of MWCNTs greatly depend on their physiochemical parameters. Metal residues in the Fe-high MWCNTs can cause high toxicity through generating ROS via the Fenton reaction when they mobilize from solid phase into metal ions in the body.^{27,28}

Because of the unusually high aspect ratio and the long-term retention time in the tissues, exposure to CNTs results in asbestos-like pathogenic behavior including inflammation and even forming granulomas. CNTs are not well recognized and cleaned by lung macrophages, and therefore may persist in the alveolar space, which facilitates their access into the systemic circulation. We speculate that CNTs may have high retention ability in the lungs with subsequent penetration into the bloodstream followed by further accumulation in multiple organs through blood circulation. The present result shows that MWCNTs still exist in the alveolar of lung tissue samples 30 days after exposure (Figure 5A). We here provide clear evidence that the MWCNTs were accumulated in different tissues including the lung, liver, kidney, and spleen at day 30 postintratracheal instillation (Figure 5), which strongly suggests that CNTs can accumulate even in the peripheral organs after passing through the lung blood–gas barrier. We speculate that this passage through the blood–gas barrier by MWCNTs may be due to leakage at the alveoli and is accompanied by persistent inflammation as seen by the increased level of the toxicity marker CC16, which is usually used to evaluate lung hyperpermeability. However, we cannot exclude the possibility that MWCNTs pass through the blood–gas barrier at an early exposure period due to acute lesions as reported.²⁹ Similarly, LDH and albumin are two other toxicity markers for alveolar epithelial barrier breakage which show great up-regulation on days 7 and 30 especially in the SH rat model. We here also have found traces of MWCNTs in liver tissues of intratracheally instilled SH rats at day 30 after exposure. More efforts should therefore be put forward to clarify the retention time, identify the target organ, and animal model sensitivity when referring to different CNT exposure routes. Until now, only a few groups have published whole-body or nose-only CNT inhalation studies because of the experimental facility and material requirements. Because of the fundamentally different characteristics of instillation and aspiration, it is hard to deliver the same precise dose with the different methods. The observed persistent bioaccumulation and subchronic toxicity of this study show that more attention should be paid to the long-term toxic effects within the lung and periphery organs that may be caused by exposure to these materials. In compromised SH rat models of cardiovascular disease, the response was much more severe and worse than in normal rats, which also calls for more safety consideration and better protection for occupationally exposed workers with potential nanomaterial exposure who should be monitored closely, particularly those with preexisting cardiovascular diseases.

CONCLUSIONS

Subchronic toxicological and cardiovascular effects were observed in SH and WKY rats at 7 and 30 days following intratracheal instillation of MWCNTs. Analysis of markers of toxicity and of cardiovascular effects showed high levels

subchronic toxicity and indirect cardiovascular damage in SH rats that are highly sensitive compared to WKY rats. Furthermore, lesions in abdominal arteries of SH rats had been found along with the long-term adverse effects due to MWCNTs exposure. These toxic effects lead to the observed cardiovascular responses including the phenotype of long-term decrease of the heart rate in this study. We here show that MWCNTs could be retained in the lung of SH rats and penetrate the lung blood–gas barrier leading to their bioaccumulation in the liver, kidney, and spleen. These results indicate that respiratory exposure to MWCNTs not only poses a great potential risk for the pulmonary system but also influences the whole cardiovascular system. The high sensitivity of SH rats suggests that individuals with existing cardiovascular diseases may be more susceptible to adverse effects following the inhalation of MWCNTs at the workplace or environment. Further investigations are necessary to resolve the underlying mechanisms and how the special physiochemical properties of MWCNTs contribute to the toxicity in MWCNT treated animals.

AUTHOR INFORMATION

Corresponding Author

*National Center for Nanoscience and Technology of China, No. 11, Beiyitia, Zhongguancun, Beijing 100190, P. R. China. Tel: +86-10-82545560. Fax: +86-10-62656765. E-mail: chenchy@nanoctr.cn.

Author Contributions

[†]R.C., L.Z., and C.G. contributed equally to this work.

Funding

This research was supported in part by the Ministry of Science and Technology of China (2011CB933401 and 2012CB934003), National Natural Science Foundation of China (21477029, 21320102003, 21277037, and 21277080), the Chinese Academy of Sciences (XDA09040400), the National Major Scientific Instruments Development Project (2011YQ03013406), International Science & Technology Cooperation Program of China, the Ministry of Science and Technology of China (2013DFG32340 and 2014DFG52500), Beijing Key Laboratory of Environmental Toxicology (2014HJDL02), Danish Council for Strategic Research grant (09-067185), Major Project of the National Social Science Fund (Grant No. 12&ZD117) “Ethical issues of high-tech,” and the National Science Fund for Distinguished Young Scholars (11425520).

Notes

The authors declare no competing financial interest.

ABBREVIATIONS

ACE, angiotensin I-converting enzyme; BALF, bronchoalveolar lavage fluid; CC16, Clara cell 16; CNTs, carbon nanotubes; CRP, C-reactive protein; ECG, electrocardiogram; ELISA, enzyme-linked immunosorbent assay; ER, endoplasmic reticulum; ET-1, endothelin-1; HE, hematoxylin–eosin; ICAM-1, intercellular adhesion molecule-1; LDH, lactate dehydrogenase; MWCNTs, multiwalled carbon nanotubes; PBS, phosphate-buffered saline; PMN, polymorphonuclear neutrophilic leukocyte; ROS, reactive oxygen species; SH, spontaneously hypertensive; SWCNTs, single-walled carbon nanotubes; TEM, transmission electron microscope; TNF- α , tumor necrosis factor- α ; vWF, von Willebrand factor; WKY, Wistar-Kyoto

REFERENCES

- (1) Nalwa, H. S., and Zhao, Y. (2007) *Nanotoxicology*, American Scientific Publishers, Valencia, CA.
- (2) Wang, P., Nie, X., Wang, Y., Li, Y., Ge, C., Zhang, L., Wang, L., Bai, R., Chen, Z., Zhao, Y., and Chen, C. (2013) Multiwall carbon nanotubes mediate macrophage activation and promote pulmonary fibrosis through TGF-beta/Smad signaling pathway. *Small* 9, 3799–3811.
- (3) Ge, C., Du, J., Zhao, L., Wang, L., Liu, Y., Li, D., Yang, Y., Zhou, R., Zhao, Y., Chai, Z., and Chen, C. (2011) Binding of blood proteins to carbon nanotubes reduces cytotoxicity. *Proc. Natl. Acad. Sci. U.S.A.* 108, 16968–16973.
- (4) Meng, L., Chen, R., Jiang, A., Wang, L., Wang, P., Li, C. Z., Bai, R., Zhao, Y., Autrup, H., and Chen, C. (2013) Short multiwall carbon nanotubes promote neuronal differentiation of PC12 cells via up-regulation of the neurotrophin signaling pathway. *Small* 9, 1786–1798.
- (5) Zhao, F., Zhao, Y., Liu, Y., Chang, X., Chen, C., and Zhao, Y. (2011) Cellular uptake, intracellular trafficking, and cytotoxicity of nanomaterials. *Small* 7, 1322–1337.
- (6) Morimoto, Y., Horie, M., Kobayashi, N., Shinohara, N., and Shimada, M. (2013) Inhalation toxicity assessment of carbon-based nanoparticles. *Acc. Chem. Res.* 46, 770–781.
- (7) Ge, C., Li, Y., Yin, J., Liu, Y., Wang, L., Zhao, Y., and Chen, C. (2012) The contributions of metal impurities and tube structure to the toxicity of carbon nanotube materials. *NPG Asia Mater.* 4, e32.
- (8) Kobayashi, N., Naya, M., Mizuno, K., Yamamoto, K., Ema, M., and Nakanishi, J. (2011) Pulmonary and systemic responses of highly pure and well-dispersed single-wall carbon nanotubes after intra-tracheal instillation in rats. *Inhalation Toxicol.* 23, 814–828.
- (9) Ingle, T., Dervishi, E., Biris, A. R., Mustafa, T., Buchanan, R. A., and Biris, A. S. (2013) Raman spectroscopy analysis and mapping the biodistribution of inhaled carbon nanotubes in the lungs and blood of mice. *J. Appl. Toxicol.* 33, 1044–1052.
- (10) Mercer, R. R., Scabilloni, J. F., Hubbs, A. F., Wang, L., Battelli, L. A., McKinney, W., Castranova, V., and Porter, D. W. (2013) Extrapulmonary transport of MWCNT following inhalation exposure. *Part. Fibre Toxicol.* 10, 38 DOI: 10.1186/1743-8977-10-38.
- (11) Brook, R. D., Rajagopalan, S., Pope, C. A., 3rd, Brook, J. R., Bhatnagar, A., Diez-Roux, A. V., Holguin, F., Hong, Y., Luepker, R. V., Mittleman, M. A., Peters, A., Siscovick, D., Smith, S. C., Jr., Whitsel, L., and Kaufman, J. D. (2010) Particulate matter air pollution and cardiovascular disease: An update to the scientific statement from the American Heart Association. *Circulation* 121, 2331–2378.
- (12) Chen, R., Huo, L., Shi, X., Bai, R., Zhang, Z., Zhao, Y., Chang, Y., and Chen, C. (2014) Endoplasmic reticulum stress induced by zinc oxide nanoparticles is an earlier biomarker for nanotoxicological evaluation. *ACS Nano* 8, 2562–2574.
- (13) Chen, R., Shi, X., Bai, R., Rang, W., Huo, L., Zhao, L., Long, D., Pui, D., and Chen, C. (2014) Airborne Nanoparticle Pollution in a Wire Electrical Discharge Machining Workshop and Potential Health Risks. *Aerosol Air Qual. Res.*, in press, DOI: 10.4209/aaqr.2014.09.0219.
- (14) Urankar, R. N., Lust, R. M., Mann, E., Katwa, P., Wang, X., Podila, R., Hilderbrand, S. C., Harrison, B. S., Chen, P., Ke, P. C., Rao, A. M., Brown, J. M., and Wingard, C. J. (2012) Expansion of cardiac ischemia/reperfusion injury after instillation of three forms of multi-walled carbon nanotubes. *Part. Fibre Toxicol.* 9, 38 DOI: 10.1186/1743-8977-9-38.
- (15) Legramante, J. M., Sacco, S., Crobeddu, P., Magrini, A., Valentini, F., Palleschi, G., Pallante, M., Balocchi, R., Iavicoli, I., Bergamaschi, A., Galante, A., Campagnolo, L., and Pietroiusti, A. (2012) Changes in cardiac autonomic regulation after acute lung exposure to carbon nanotubes: Implications for occupational exposure. *J. Nanomater.* 2012, 1–9.
- (16) Ge, C., Li, W., Li, Y., Li, B., Du, J., Qiu, Y., Liu, Y., Gao, Y., Chai, Z., and Chen, C. (2011) Significance and systematic analysis of metallic impurities of carbon nanotubes produced by different manufacturers. *J. Nanosci. Nanotechnol.* 11, 2389–2397.

- (17) Datsyuk, V., Kalyva, M., Papagelis, K., Parthenios, J., Tasis, D., Siokou, A., Kallitsis, I., and Galiotis, C. (2008) Chemical oxidation of multiwalled carbon nanotubes. *Carbon* 46, 833–840.
- (18) Wang, X., Xia, T., Duch, M. C., Ji, Z., Zhang, H., Li, R., Sun, B., Lin, S., Meng, H., Liao, Y. P., Wang, M., Song, T. B., Yang, Y., Hersam, M. C., and Nel, A. E. (2012) Pluronic F108 coating decreases the lung fibrosis potential of multiwall carbon nanotubes by reducing lysosomal injury. *Nano Lett.* 12, 3050–3061.
- (19) Ge, C., Meng, L., Xu, L., Bai, R., Du, J., Zhang, L., Li, Y., Chang, Y., Zhao, Y., and Chen, C. (2012) Acute pulmonary and moderate cardiovascular responses of spontaneously hypertensive rats after exposure to single-wall carbon nanotubes. *Nanotoxicology* 6, 526–542.
- (20) Gordon, C. J., Schladweiler, M. C., Krantz, T., King, C., and Kodavanti, U. P. (2012) Cardiovascular and thermoregulatory responses of unrestrained rats exposed to filtered or unfiltered diesel exhaust. *Inhalation Toxicol.* 24, 296–309.
- (21) Liu, Y., Zhao, Y., Sun, B., and Chen, C. (2013) Understanding the toxicity of carbon nanotubes. *Acc. Chem. Res.* 46, 702–713.
- (22) Erdely, A., Hulderman, T., Salmen, R., Liston, A., Zeidler-Erdely, P. C., Schwegler-Berry, D., Castranova, V., Koyama, S., Kim, Y. A., Endo, M., and Simeonova, P. P. (2009) Cross-talk between lung and systemic circulation during carbon nanotube respiratory exposure. Potential biomarkers. *Nano Lett.* 9, 36–43.
- (23) Najjar, S. S., Scuteri, A., and Lakatta, E. G. (2005) Arterial aging: is it an immutable cardiovascular risk factor? *Hypertension* 46, 454–462.
- (24) Lao, F., Chen, L., Li, W., Ge, C., Qu, Y., Sun, Q., Zhao, Y., Han, D., and Chen, C. (2009) Fullerene nanoparticles selectively enter oxidation-damaged cerebral microvessel endothelial cells and inhibit JNK-related apoptosis. *ACS Nano* 3, 3358–3368.
- (25) Lao, F., Li, W., Han, D., Qu, Y., Liu, Y., Zhao, Y., and Chen, C. (2009) Fullerene derivatives protect endothelial cells against NO-induced damage. *Nanotechnology* 20, 225103.
- (26) Suzuki, K., Masawa, N., and Takatama, M. (2001) The pathogenesis of cerebrovascular lesions in hypertensive rats. *Med. Electron Microsc.* 34, 230–239.
- (27) Isobe, H., Tanaka, T., Maeda, R., Noiri, E., Solin, N., Yudasaka, M., Iijima, S., and Nakamura, E. (2006) Preparation, purification, characterization, and cytotoxicity assessment of water-soluble, transition-metal-free carbon nanotube aggregates. *Angew. Chem., Int. Ed.* 45, 6676–6680.
- (28) Meng, L., Jiang, A., Chen, R., Li, C. Z., Wang, L., Qu, Y., Wang, P., Zhao, Y., and Chen, C. (2013) Inhibitory effects of multiwall carbon nanotubes with high iron impurity on viability and neuronal differentiation in cultured PC12 cells. *Toxicology* 313, 49–58.
- (29) Stapleton, P. A., Minarchick, V. C., Cumpston, A. M., McKinney, W., Chen, B. T., Sager, T. M., Frazer, D. G., Mercer, R. R., Scabilloni, J., Andrew, M. E., Castranova, V., and Nurkiewicz, T. R. (2012) Impairment of coronary arteriolar endothelium-dependent dilation after multi-walled carbon nanotube inhalation: a time-course study. *Int. J. Mol. Sci.* 13, 13781–13803.